Original Article

Exploring the therapeutic potential of simvastatin in pancreatic neuroendocrine neoplasms: insights into cell cycle regulation and apoptosis

Xiao-Ting Shi[#]^, Li-Jun Yan[#], Fei-Yu Lu[#], Mu-Jie Ye, Ping Yu, Yuan Zhong, Jin-Hao Chen, Chun-Hua Hu, Qi-Yun Tang

Department of Geriatric Gastroenterology, Neuroendocrine Tumor Center, Jiangsu Province Hospital, The First Affiliated Hospital of Nanjing Medical University, Institute of Neuroendocrine Tumor, Nanjing Medical University, Nanjing, China

Contributions: (I) Conception and design: XT Shi, MJ Ye; (II) Administrative support: QY Tang; (III) Provision of study materials or patients: LJ Yan; (IV) Collection and assembly of data: XT Shi, P Yu, FY Lu; (V) Data analysis and interpretation: Y Zhong, JH Chen, CH Hu; (VI) Manuscript writing: All authors; (VII) Final approval of manuscript: All authors.

[#]These authors contributed equally to this work.

Correspondence to: Qi-Yun Tang, MD, Department of Geriatric Gastroenterology, Neuroendocrine Tumor Center, Jiangsu Province Hospital, The First Affiliated Hospital of Nanjing Medical University, Institute of Neuroendocrine Tumor, Nanjing Medical University, No. 300 Guangzhou Road, Nanjing 210029, China. Email: tqy831@163.com.

Background: Pancreatic neuroendocrine neoplasm (pNEN) poses significant challenges in clinical management due to their heterogeneity and limited treatment options. In this study, we investigated the potential of simvastatin (SIM) as an anti-tumor agent in pNEN.

Methods: We conducted cell culture experiments using QGP-1 and BON-1 cell lines and assessed cell viability, proliferation, migration, and invasion following SIM treatment. To further validate our findings, we performed *in vivo* experiments using a mouse xenograft model. Additionally, we investigated the underlying molecular mechanisms by analyzing changes in cell cycle progression, apoptosis, and signaling pathways.

Results: SIM treatment suppresses pNEN growth both *in vitro* and *in vivo*, and led to G1 phase arrest in QGP-1 cells. In contrast, SIM affected both the G1-S and G2-M phase transitions in the BON-1 cell line and induced apoptosis, indicating diverse mechanisms of action. Furthermore, SIM treatment resulted in decreased expression of mutant p53 (mutp53) in BON-1 cells, suggesting a potential therapeutic strategy targeting mutp53. Modulation of the MAPK pathway was also implicated in QGP-1 cells.

Conclusions: Our study highlights SIM as a promising candidate for pNEN treatment by inducing cell cycle arrest or apoptosis, potentially through the p53 and MAPK pathways. Further research is warranted to fully elucidate SIM's mechanisms of action and evaluate its therapeutic potential in clinical settings.

Keywords: Pancreatic neuroendocrine tumor; simvastatin (SIM); p53; MAPK

Submitted Mar 06, 2024. Accepted for publication Jun 25, 2024. Published online Aug 12, 2024.
doi: 10.21037/tcr-24-363
View this article at: https://dx.doi.org/10.21037/tcr-24-363

Introduction

Pancreatic neuroendocrine neoplasm (pNEN) is a type of pancreatic neoplasm originating from neuroendocrine cells (1). Its incidence rate is approximately 0.48 per 100,000 persons [2000–2012] and has shown a significant increase in recent years (2).

Due to substantial heterogeneity, managing pNEN is highly complex. Surgical resection remains the primary

^ ORCID: 0009-0001-5759-5717.

option for localized pNEN, while debulking surgery is recommended for locally advanced cases (3). For unresectable progressive disease, medical therapies such as somatostatin analogs, everolimus, temozolomide-based and streptozotocin-based chemotherapies, radiation therapy, and immunotherapy may prolong survival (4,5). However, the severe side effects and prolonged treatment duration compared to surgery pose challenges, leaving the treatment of advanced pNEN an unmet clinical need (6).

Statins are a class of hydroxymethylglutaryl-coenzyme A reductase (HMGCR) inhibitor drugs that block the mevalonate pathway and are commonly used as cholesterol-lowering agents (7). Recent studies have indicated their potential in cancer treatment and prevention (8,9). Among statins, simvastatin (SIM) has garnered significant attention for its protective effect against cancer and its ability to enhance chemotherapy's adjuvant efficacy, particularly in breast and colon cancer in clinical studies (10-14). Multiple studies have demonstrated SIM's anti-tumor effects in various types of tumors, including suppressing cell proliferation and migration (15), inducing cell cycle arrest (16,17) and inhibiting tumor angiogenesis (18,19). Published researches by our group revealed that lipid metabolism is related to pNEN progression (20,21). As a prominent lipid-lowering agent, the potential anti-tumor effects of SIM on PNEN merit detailed investigation.

In this study, we assessed SIM's anti-tumor effect in pNEN cells, elucidating its mechanisms via the MAPK pathway-mediated proliferation retardation, cell-cycle arrest, or apoptosis in pNEN cells for the first time. Our findings suggest that SIM may significantly contribute to tumor suppression, and targeting the p53 and MAPK pathway could be promising therapeutic strategies for pNEN treatment. We present this article in accordance with the MDAR and ARRIVE reporting checklists (available at https://tcr.amegroups.com/article/view/10.21037/tcr-24-363/rc).

Highlight box

Key findings

- Simvastatin (SIM) inhibits the proliferation and metastasis of pancreatic neuroendocrine neoplasm (pNEN) by inducing cell cycle and apoptosis, potentially through the p53 and MAPK pathways.

What is known and what is new?

- SIM has been reported to play a beneficial role in various cancer types in a variety of ways.
- SIM is a promising drug and the p53 and MAPK pathways are potential targets for pNEN treatment.

What is the implication, and what should change now?

- We found a new treatment for pNEN, and further research is warranted to fully elucidate SIM's mechanisms of action and evaluate its therapeutic potential in clinical settings.

Methods

Cell culture

The human pancreatic neuroendocrine tumor cancer cell line QGP-1 (JCRB0183) was obtained from the JCRB cell bank (JCRB0183), and BON-1 cells were a gift from Xianrui Yu of Fudan University Affiliated Cancer Hospital. QGP-1 cells were cultured in RPMI 1640 (Gibco, USA), and BON-1 cells were cultured in DMEM/F-12, both supplemented with 10% fetal bovine serum (FBS; Gibco) and 1% penicillin-streptomycin (NCM Biotech, China). Cells were maintained in a humidified atmosphere containing 5% CO_2 at 37 ℃.

Drugs, chemicals and reagents

SIM was purchased from Macklin (Shanghai, China) and dissolved in dimethylsulfoxide (DMSO; Sigma, Germany) to obtain a concentration of 100 mM (mmol/L). All treatments were diluted in cell culture medium to achieve final concentrations before use, with a maximum of 0.5 μL of DMSO per ml of culture medium. Matrigel was obtained from BD Biosciences (New Jersey, USA). Antibodies used for Western blot analysis were as follows: CDK2 (#2546), CDK6 (#3136), CDK4 (#12790), p21 (#64016), GAPDH (#5174), PARP (#9542), Caspase3 (#9662), BAX (#2772), BCL-2 (#15071), p44/42 MAPK (Erk1/2) (#9102), phospho-p44/42 MAPK (Erk1/2) (#9102) from Cell Signaling Technology (Boston, USA); cyclin D1 (#sc-8396), cyclin E (#sc-248) from Santa Cruz (California, USA); KLF4 (ab215036) from Abcam (Cambridge, UK). HRP-linked anti-rabbit (#7074) and anti-mouse (#7076) secondary antibodies were obtained from Cell Signaling Technology.

Cell proliferation assay

Cell proliferation was assessed using the Cell Counting Kit-8 (CCK-8; Dojindo, Japan) and the 5-ethynyl-2'-deoxyuridine (EdU) kit (Ribobio, Guangzhou, China) according to the manufacturer's instructions.

CCK-8 assay: QGP-1 cells were treated with 40 μM (μmol/L) SIM for 48 h. Subsequently, cells were inoculated into 96-well plates at a density of 5,000 cells/well with 3 replicates per well. After treatment with CCK8 reagent for 2 h, the absorbance at 450 nm was monitored, continuously for 4 days.

EdU labeling assay: QGP-1 cells were seeded at a density of 4×10^4 cells/well in 96-well plates. Cells were treated with 50 μM EdU in medium at 37 ℃ for 2 hours. Subsequently, the cells were fixed in 4% paraformaldehyde. After permeabilization with 0.5% Triton X-100, they were treated with 1× Apollo reaction cocktail for 30 minutes. Finally, the cells were stained with 1× Hoechst 33342 for 30 minutes to visualize the DNA content, and observed using a fluorescence microscope (Zeiss, Oberkochen, Germany).

Colony formation assay

After treatment of 40 μM SIM for 48 hours, cells were seeded onto new 6-well plates at a density of 2,000 cells per well. QGP-1 cells and BON-1 cells were cultured for approximately 14 days until colonies were large enough to be clearly distinguished. The cells were then fixed with methanol and stained with crystal violet.

Migration and invasion assays

The ability of cell migration and invasion were evaluated by transwell (Corning, New York, USA) assay. After 48 hours of SIM treatment, QGP-1 and BON-1 cells were resuspended in 0.5 mL serum free medium and added to the upper chamber with either an uncoated or Matrigel (BD Biosciences) coated membrane; medium containing 20% FBS was added to the lower chamber. In order to minimize the effect of apoptosis on this experiment, we counted the number of viable cells. After incubation for 48 h, migrated or invaded cells were fixed with methanol and stained with crystal violet (Beyotime, Shanghai, China), and were counted in 5 random selected fields per sample.

Western blotting

Cells were lysed in RIPA Lysing Buffer (Beyotime) supplemented with PMSF (Sunshine Biotech, Co., Ltd., Guangzhou, China). The protein concentration was determined using a BCA Protein Assay Kit (Beyotime). SDS-PAGE was performed with 10% acrylamide gels, and proteins were transferred to PVDF membranes (Millipore, Boston, USA) using a semidry transfer system (Bio-Rad, California, USA). Membranes were incubated in TBST (Tris Buffered Saline containing 0.1% Tween-20) with 5% nonfat dry milk for 2 hours at room temperature. Primary antibodies were then incubated at 4 ℃ overnight, followed by appropriate HRP-conjugated secondary antibodies. The protein bands were visualized using an ECL system (Biosharp, China).

Cell cycle and apoptosis analysis

QGP-1 cells were collected and seeded into 6-well plates at a density of 5×10^5 cells per dish, then maintained for 24 hours. Next, cells were treated with 40 μM SIM for 48 hours. Cell cycle analysis was conducted using the Cell Cycle Staining Kit (Vazyme, Nanjing, China). Briefly, cells are first fixed with 75% ethanol and stored overnight at –20 ℃. For analysis, the cells are rehydrated with PBS and stained with 1 mL of DNA staining solution after removal of PBS. Apoptosis assay was detected using the Annexin V-FITC/PI Apoptosis Detection Kit A211 (APExBIO, Houston, USA). Cell cycle distribution and apoptosis assay were determined using a flow cytometer (Gallios, California, USA).

Functional and pathway enrichment analyses

Total RNA was isolated and purified using TRIzol reagent (Invitrogen, California, USA). From 1 μg of total RNA, poly(A) RNA was selectively captured using Dynabeads Oligo(dT)25-61005 (Thermo Fisher Scientific, Waltham, USA). This poly(A) RNA was then fragmented into small pieces, and the cleaved RNA fragments were reverse transcribed to synthesize cDNA. The cDNA was subsequently amplified to produce fragments of approximately 300±50 bp. For RNA sequencing analysis, the Kyoto Encyclopedia of Genes and Genomes (KEGG) signaling pathway database was used to analyze the signaling pathway enrichment of differentially expressed genes in the SIM-treated group compared with the control. A threshold of $|\log2FC| \geq 1$ and $P<0.05$ were used as screening conditions.

Tumor xenograft model in nude mice

Athymic male BALB/c nude mice (4 weeks old) were obtained from the Animal Center of Nanjing Medical University. QGP-1 cells (5×10^6 cells/mice) were resuspended in 100 μL serum-free medium and injected subcutaneously into the right flank of mice. Mice received normal saline

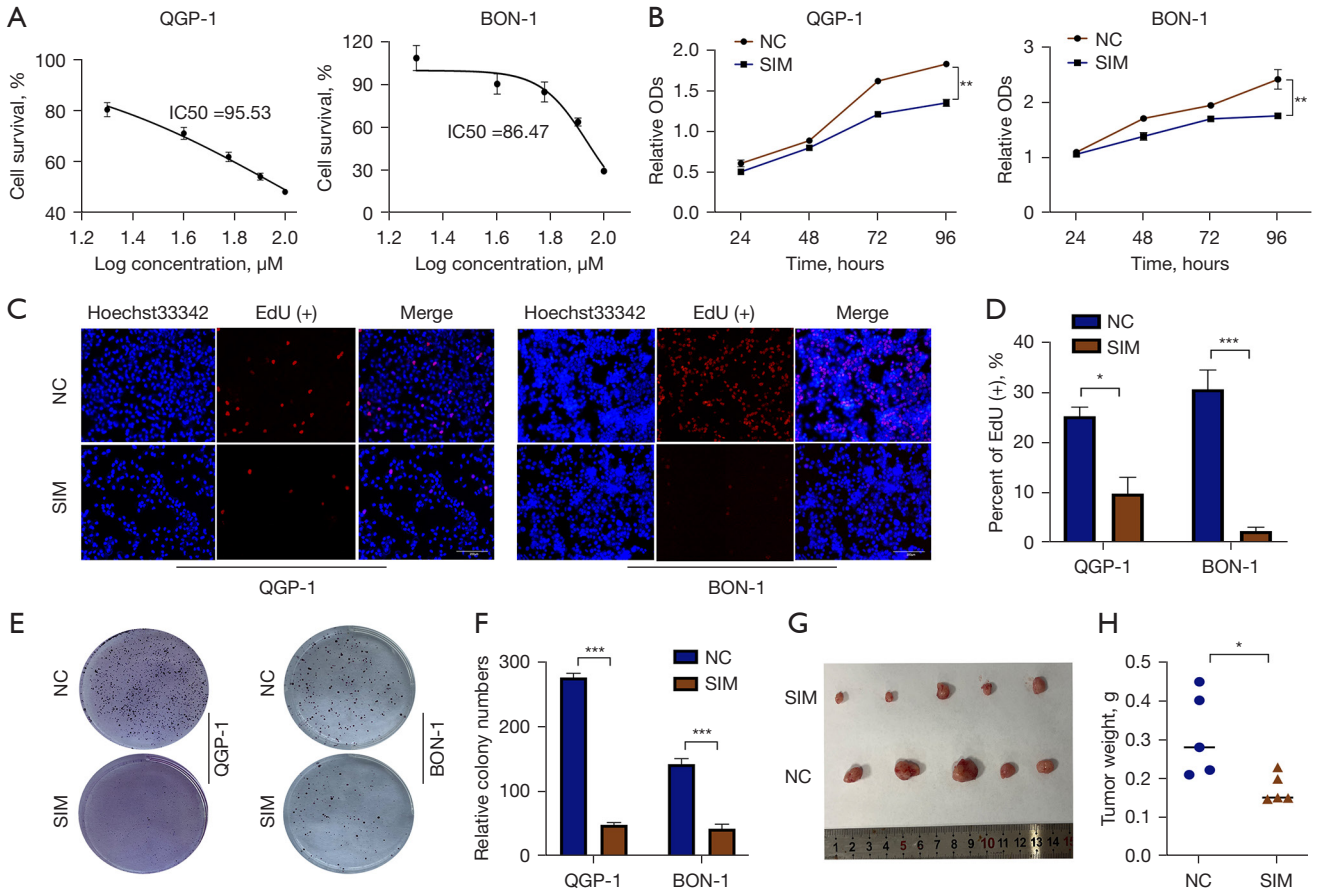

Figure 1 SIM suppressed pNEN cells viability and proliferation. (A) IC50 values of QGP-1 cells and BON-1 cells treated with SIM for 48 hours. The 95% CI for QGP-1 cells is 89.28–103.4, while for BON-1 cells, the 95% CI is 81.60–91.97. (B-F) Both cell lines' growth rates were determined with CCK-8 proliferation assay, EdU labelling analysis. and colony formation assay. (E) Cells were stained with crystal violet. (G,H) Representative images of the tumors formed in nude mice. The scale bar in Figure C is 200 μm. *, P<0.05; **, P<0.01; ***, P<0.001. NC, negative control; SIM, simvastatin; pNEN, pancreatic neuroendocrine neoplasms; IC50, half maximal inhibitory concentration; CI, confidence interval; CCK-8, Cell Counting Kit-8; EdU, 5-ethynyl-2'-deoxyuridine.

(10 mg/kg) or SIM (10 mg/kg) orally once daily until 4 weeks after cell injection, with 5 mice in each group. Tumors were then excised and weighed. Tumor volumes were calculated using the formula: 0.5 × length × width^2. All animal experiments were performed under a project license (No. IACUC-2208028) granted by Institutional Animal Care and Use Committee of Nanjing Medical University, in compliance with Chinese national or institutional guidelines for the care and use of animals.

Statistical analysis

All statistical analyses were performed using GraphPad Prism 9 software (GraphPad Software, La Jolla, California, USA). Two-group comparisons were analyzed with an unpaired *t*-test, and P values were calculated. Each experiment was repeated at least three times, with three replicates set up each time, and similar results were obtained. P<0.05 was considered to be statistically significant.

Results

SIM suppresses pNEN growth both in vitro and in vivo

The 48-hour IC50 cytotoxicity values of SIM are shown in *Figure 1A*. Based on these results, a concentration of 40 μM SIM was chosen for further experiments with QGP-1 cells and BON-1 cells, and an incubation time of 48 hours was

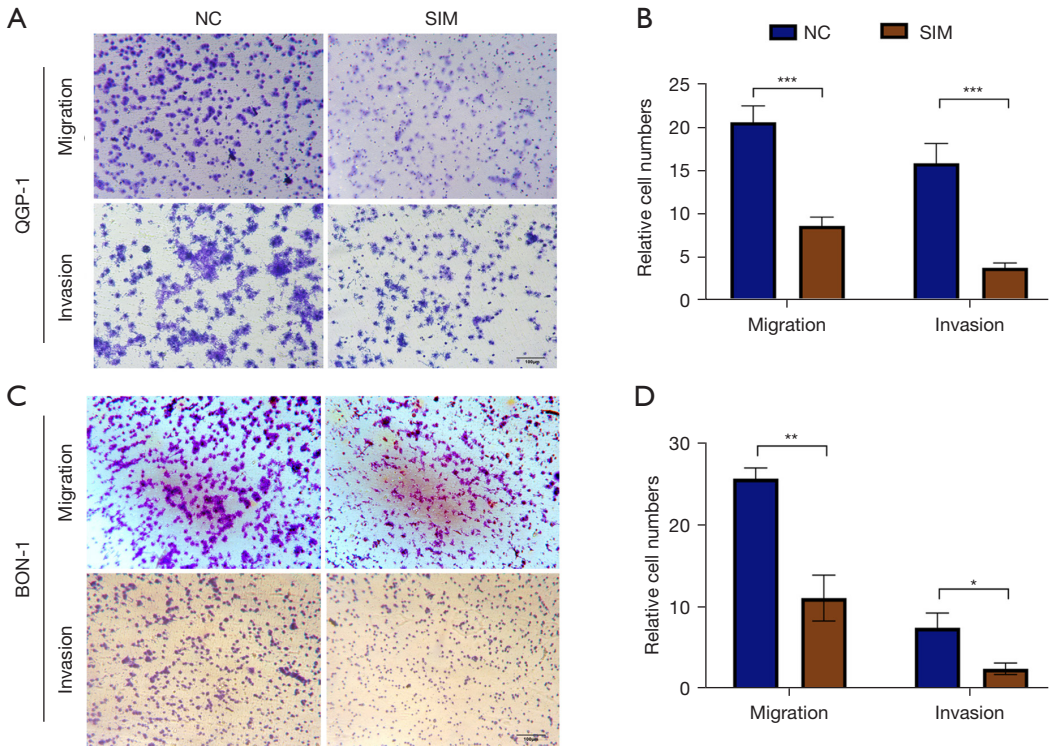

Figure 2 SIM reduces pNEN cells migration and invasion. (A,B) Significant reduction in cell migration and cell invasion was found in SIM-treated group in QGP-1 cells. (C,D) A comparable reduction in migration and invasion was observed in BON-1cells. Cells were stained with crystal violet. The scale bar in (A,C) is 100 μm. *, P<0.05; **, P<0.01; ***, P<0.001. NC, negative control; SIM, simvastatin; pNEN, pancreatic neuroendocrine neoplasms.

selected. CCK-8 assay (*Figure 1B*), EdU assays (*Figure 1C,1D*), and colony formation assay (*Figure 1E,1F*) revealed that SIM significantly reduced cell growth. In the *in vivo* experiment, tumors formed in the SIM-treated group were smaller than those in the control group (*Figure 1G,1H*).

SIM reduces pNEN cells migration and invasion

The transwell migration assay showed that the SIM-treated group had fewer migrated cells in both cell lines compared with the control group. Similar results were noted in the transwell invasion assay (*Figure 2A-2D*).

SIM promotes cell-cycle arrest in QGP-1 cells and apoptosis in BON-1 cells

Previous studies have revealed the cell cycle blocking effect of SIM in other tumors. We analyzed the cell-cycle distribution of QGP-1 and BON-1 cells by flow cytometry after 48-hour exposure to SIM. In QGP-1 cells, SIM increased the number of cells in G1 phase and decreased the number in G2 phase, indicating that the cells underwent G1 cycle arrest. In BON-1 cells, SIM increased the number of cells in G1 and G2 phases and decreased cell number in S phase, indicating affected conversion of G1-S and G2-M phases (*Figure 3A,3B*).

We also assessed the percentage of apoptotic cells by flow cytometric analysis. In BON-1 cells, the dot-plot analysis indicated a significant increase in apoptotic cells in the SIM-treated group compared with control. Conversely, no significant increase in apoptotic cells was observed in QGP-1 cells after SIM treatment (*Figure 3C,3D*).

Furthermore, we examined the expression of cell cycle regulators and apoptosis related regulators. As shown in *Figure 3E*, when treated with SIM, the expressions of cyclin D1, cyclin E2, CDK2 were obviously inhibited, whereas p21 was over expressed in QGP-1 cells, indicating that SIM inhibits QGP-1 cell proliferation partially through inducing cell-cycle arrest. While in BON-1 cells, we only observed corresponding changes in CDK2 and CDK6.

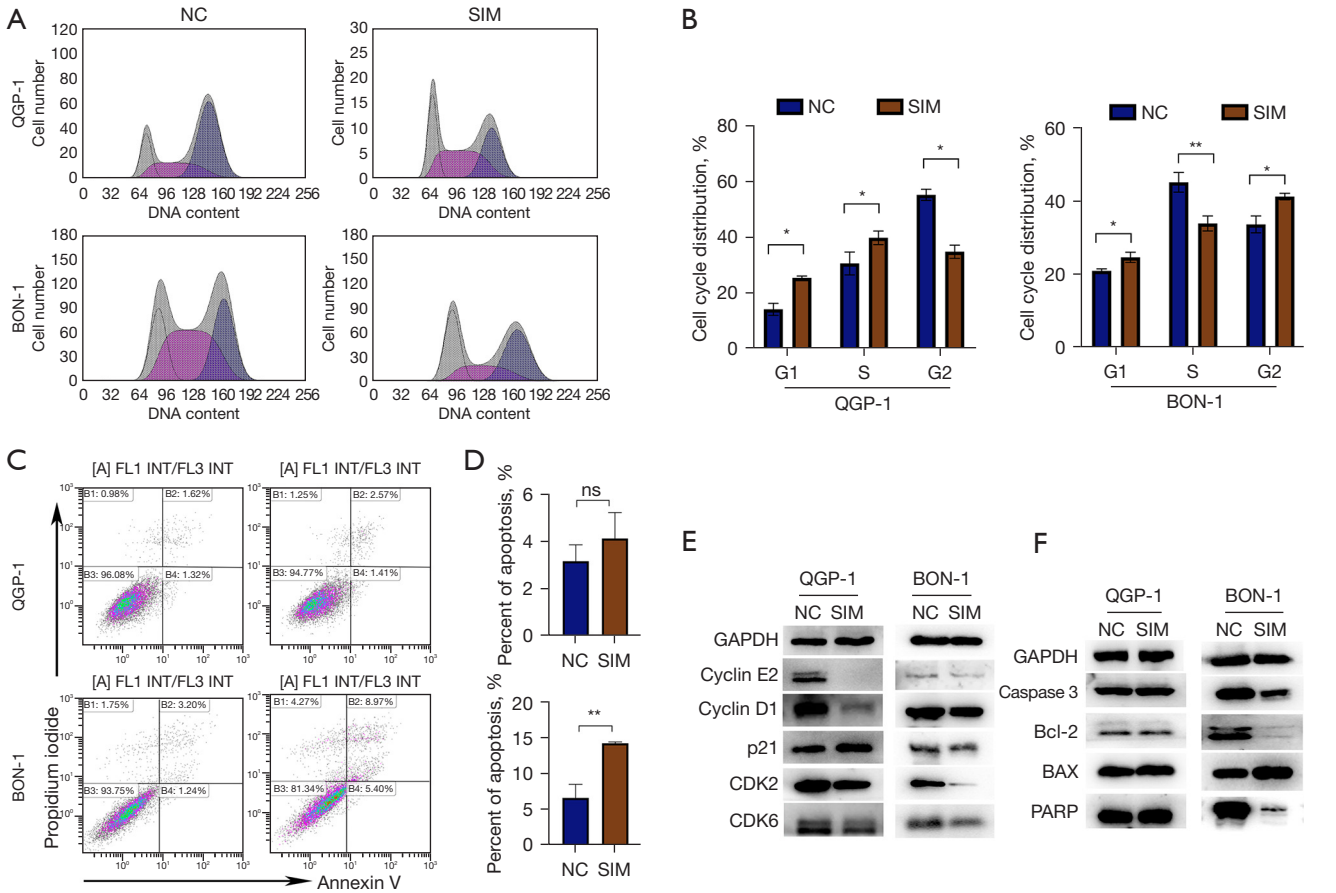

Figure 3 SIM induces accumulation of G1 phase in QGP-1 cells and apoptosis in BON-1 cells. (A,B) Flow cytometry analysis of Cell-cycle distribution in both cell lines. (C,D) Flow cytometry analysis of the apoptotic cells using Annexin V/PI double-staining assay. (E,F) Western blot analysis of the protein expression of cell-cycle and apoptotic regulators. ns, P>0.05; *, P<0.05; **, P<0.01. NC, negative control; SIM, simvastatin; PI, propidium iodide.

Consistent with the fact that apoptosis of BON-1 cells increased after SIM treatment, the apoptosis related regulators including PARP, Caspase 3, BCL-2 were decreased, and BAX was over-expressed (*Figure 3F*), suggesting that SIM inhibits BON-1 cells proliferation through inducing cell apoptosis.

SIM suppresses BON-1 cells growth via p53 pathway and QGP-1 cells via MAPK pathway

The KEGG enrichment results showed p53 pathway and MAPK signaling pathway as the enriched signaling pathways (*Figure 4A*). We found that p53 was hardly detected in QGP-1 cells, but highly expressed in BON-1 cells, and that p53 decreased significantly after treated with SIM in BON-1 cells (*Figure 4B*). It suggested that mutant p53 may be expressed in BON-1 cells, and SIM suppressed BON-1 cells growth by targeting the functions of mutant p53. While in QGP-1 cells, pERK was significantly inhibited after treatment of SIM (*Figure 4C*), indicating that SIM inhibited QGP-1 cells growth through modulation of the MAPK pathway.

Discussion

pNEN represent a heterogeneous tumor subtype with varied clinical manifestations, behavior, and prognosis (22). Despite advancements in treatment modalities, effective therapies for pNEN remain elusive, highlighting the need for novel drugs to control tumor growth. In our study, we investigated the potential of SIM as an anti-tumor agent in pNEN cells.

Statins, including SIM, exert their effects by inhibiting

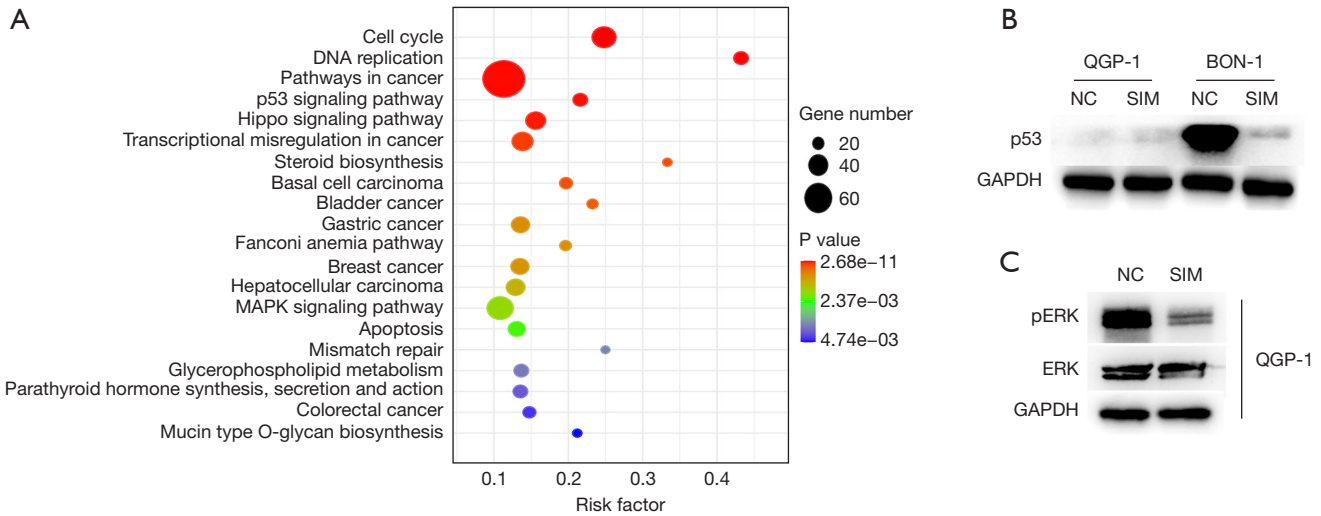

Figure 4 KEGG pathway enrichment showed the related signaling pathways. (A) The abscissa represents the ratio of enriched genes, and the ordinate represents pathways. The color gradient from red to blue indicates P value changes from small to large after correction. (B) P53 is highly expressed in BON-1 cells, but hardly detected in QGP-1 cells, and after SIM treatment, p53 decreased significantly in BON-1 cells. (C) In QGP-1 cells, pERK was inhibited after treatment of SIM. KEGG, Kyoto Encyclopedia of Genes and Genomes; NC, negative control; SIM, simvastatin.

HMGCR, a key enzyme in the mevalonate pathway. This pathway regulates the production of downstream metabolites involved in diverse cellular functions, including cell signaling and proliferation (23). Consistent with previous research (16,17,24), our findings demonstrated that SIM induced cell cycle arrest in pNEN cells, with distinct effects observed in different cell lines. Specifically, SIM treatment led to G1 phase arrest in QGP-1 cells, accompanied by downregulation of cyclin D1/CDK6 and cyclin E/CDK2, key regulators of the G1-S transition. As we know, G1 cyclins (cyclin D and cyclin E) bind to cyclin-dependent kinases (CDKs) 4/6 and CDK2, respectively, initiating the G1-S transition (25). Our findings corroborate these observations, as SIM treatment led to G1 phase arrest in QGP-1 cells; while in BON-1 cell line, both of the G1-S and G2-M phases conversion were affected. Besides, in BON-1 cell line, SIM treatment resulted in increased apoptosis marked by modulation of apoptosis-related proteins, suggesting different mechanisms of action in inhibiting proliferation between the two cell types.

P53, a well-studied tumor suppressor protein, is frequently mutated in various tumor types, leading to loss of its wild-type activity (26). Mutant p53 (mutp53) plays a crucial role in cancer progression and therapy resistance (27). The important role of mutp53 in cancer makes it an attractive therapeutic target. A large number of drugs have been identified or designed to rescue mutp53 and reactivate its anti-tumor ability through various mechanisms (28). Our study revealed high p53 expression in BON-1 cells, suggesting the presence of mutp53. The substantial decrease in p53 expression following SIM treatment provides compelling evidence of SIM's potential to target mutp53 effectively. By reducing mutp53 levels, SIM may disrupt the oncogenic functions associated with mutp53 and promote apoptosis in BON-1 cells. Overall, our findings support the notion that SIM has the ability to target and modulate mutp53 expression, thereby presenting a promising therapeutic avenue for combating mutp53-driven cancers. Further investigation into the specific mechanisms underlying SIM's interaction with mutp53, as well as its broader effects on cancer progression and therapy resistance, is warranted to fully elucidate its potential as a mutp53-targeted therapy.

The MAPK pathway has been implicated in modulating drug sensitivity and resistance in cancers (29). Studies have shown that ERK1/2, a key component of the MAPK pathway, promotes cell cycle progression from G1 to S phase (30) and increases the expression of pivotal cell cycle control molecules such as cyclin D1/E1 and E2F1 (31). Our findings suggest a potential role of the MAPK pathway in mediating SIM-induced cell cycle arrest in QGP-1 cells, warranting further investigation into the molecular

mechanisms involved.

Conclusions

In summary, our study reveals that SIM inhibits pNEN cells proliferation by inducing cell cycle arrest or apoptosis potentially through the p53 and MAPK pathway. These results highlight SIM as a promising candidate for the treatment of pNEN and underscore the importance of further investigations to elucidate its precise mechanisms of action and therapeutic potential in clinical settings.

Acknowledgments

Funding: This work was supported by the Science Foundation Project of Ili & Jiangsu Joint Institute of Health (grant No. yl2020lhms05) and Wuxi "Taihu talent plan" for the excellent medical expert team (grant No. 2021-9).

Footnote

Reporting Checklist: The authors have completed the MDAR and ARRIVE reporting checklists. Available at https://tcr.amegroups.com/article/view/10.21037/tcr-24-363/rc

Data Sharing Statement: Available at https://tcr.amegroups.com/article/view/10.21037/tcr-24-363/dss

Peer Review File: Available at https://tcr.amegroups.com/article/view/10.21037/tcr-24-363/prf

Conflicts of Interest: All authors have completed the ICMJE uniform disclosure form (available at https://tcr.amegroups.com/article/view/10.21037/tcr-24-363/coif). The authors have no conflicts of interest to declare.

Ethical Statement: The authors are accountable for all aspects of the work in ensuring that questions related to the accuracy or integrity of any part of the work are appropriately investigated and resolved. Experiments were performed under a project license (No. IACUC-2208028) granted by Institutional Animal Care and Use Committee of Nanjing Medical University, in compliance with Chinese national or institutional guidelines for the care and use of animals.

References

1. Li X, Gou S, Liu Z, et al. Assessment of the American Joint Commission on Cancer 8th Edition Staging System for Patients with Pancreatic Neuroendocrine Tumors: A Surveillance, Epidemiology, and End Results analysis. Cancer Med 2018;7:626-34.
2. Dasari A, Shen C, Halperin D, et al. Trends in the Incidence, Prevalence, and Survival Outcomes in Patients With Neuroendocrine Tumors in the United States. JAMA Oncol 2017;3:1335-42.
3. Ma ZY, Gong YF, Zhuang HK, et al. Pancreatic neuroendocrine tumors: A review of serum biomarkers, staging, and management. World J Gastroenterol 2020;26:2305-22.
4. Scott AT, Howe JR. Evaluation and Management of Neuroendocrine Tumors of the Pancreas. Surg Clin North Am 2019;99:793-814.
5. Perri G, Prakash LR, Katz MHG. Pancreatic neuroendocrine tumors. Curr Opin Gastroenterol 2019;35:468-77.
6. Mpilla GB, Philip PA, El-Rayes B, et al. Pancreatic neuroendocrine tumors: Therapeutic challenges and research limitations. World J Gastroenterol 2020;26:4036-54.
7. Juarez D, Fruman DA. Targeting the Mevalonate Pathway in Cancer. Trends Cancer 2021;7:525-40.
8. Zhong S, Zhang X, Chen L, et al. Statin use and mortality in cancer patients: Systematic review and meta-analysis of observational studies. Cancer Treat Rev 2015;41:554-67.
9. Duarte JA, de Barros ALB, Leite EA. The potential use of simvastatin for cancer treatment: A review. Biomed Pharmacother 2021;141:111858.
10. Graaf MR, Beiderbeck AB, Egberts AC, et al. The risk of cancer in users of statins. J Clin Oncol 2004;22:2388-94.
11. Cauley JA, Zmuda JM, Lui LY, et al. Lipid-lowering drug use and breast cancer in older women: a prospective study. J Womens Health (Larchmt) 2003;12:749-56.
12. Higgins MJ, Prowell TM, Blackford AL, et al. A short-term biomarker modulation study of simvastatin in women

at increased risk of a new breast cancer. Breast Cancer Res Treat 2012;131:915-24.
13. Yulian ED, Siregar NC, Sudijono B, et al. The role of HMGCR expression in combination therapy of simvastatin and FAC treated locally advanced breast cancer patients. Breast Dis 2023;42:73-83.
14. Lee J, Hong YS, Hong JY, et al. Effect of simvastatin plus cetuximab/irinotecan for KRAS mutant colorectal cancer and predictive value of the RAS signature for treatment response to cetuximab. Invest New Drugs 2014;32:535-41.
15. Wang F, Liu W, Ning J, et al. Simvastatin Suppresses Proliferation and Migration in Non-small Cell Lung Cancer via Pyroptosis. Int J Biol Sci 2018;14:406-17.
16. Wang G, Cao R, Wang Y, et al. Simvastatin induces cell cycle arrest and inhibits proliferation of bladder cancer cells via PPARγ signalling pathway. Sci Rep 2016;6:35783.
17. Chen MJ, Cheng AC, Lee MF, et al. Simvastatin induces G(1) arrest by up-regulating GSK3β and down-regulating CDK4/cyclin D1 and CDK2/cyclin E1 in human primary colorectal cancer cells. J Cell Physiol 2018;233:4618-25.
18. Rao PS, Rao US. Statins decrease the expression of c-Myc protein in cancer cell lines. Mol Cell Biochem 2021;476:743-55.
19. Li G, Zheng J, Xu B, et al. Simvastatin inhibits tumor angiogenesis in HER2-overexpressing human colorectal cancer. Biomed Pharmacother 2017;85:418-24.
20. Chen J, Ye M, Bai J, et al. ALKBH5 enhances lipid metabolism reprogramming by increasing stability of FABP5 to promote pancreatic neuroendocrine neoplasms progression in an m6A-IGF2BP2-dependent manner. J Transl Med 2023;21:741.
21. Lu F, Ye M, Hu C, et al. FABP5 regulates lipid metabolism to facilitate pancreatic neuroendocrine neoplasms progression via FASN mediated Wnt/β-catenin pathway. Cancer Sci 2023;114:3553-67.
22. Gao L, Natov NS, Daly KP, et al. An update on the management of pancreatic neuroendocrine tumors. Anticancer Drugs 2018;29:597-612.
23. Guerra B, Recio C, Aranda-Tavío H, et al. The Mevalonate Pathway, a Metabolic Target in Cancer Therapy. Front Oncol 2021;11:626971.
24. Wang ST, Ho HJ, Lin JT, et al. Simvastatin-induced cell cycle arrest through inhibition of STAT3/SKP2 axis and activation of AMPK to promote p27 and p21 accumulation in hepatocellular carcinoma cells. Cell Death Dis 2017;8:e2626.
25. Sherr CJ, Roberts JM. Inhibitors of mammalian G1 cyclin-dependent kinases. Genes Dev 1995;9:1149-63.
26. Muller PA, Vousden KH. Mutant p53 in cancer: new functions and therapeutic opportunities. Cancer Cell 2014;25:304-17.
27. Sabapathy K, Lane DP. Therapeutic targeting of p53: all mutants are equal, but some mutants are more equal than others. Nat Rev Clin Oncol 2018;15:13-30.
28. Li Y, Wang Z, Chen Y, et al. Salvation of the fallen angel: Reactivating mutant p53. Br J Pharmacol 2019;176:817-31.
29. Lee S, Rauch J, Kolch W. Targeting MAPK Signaling in Cancer: Mechanisms of Drug Resistance and Sensitivity. Int J Mol Sci 2020;21:1102.
30. Zerrad-Saadi A, Lambert-Blot M, Mitchell C, et al. GH receptor plays a major role in liver regeneration through the control of EGFR and ERK1/2 activation. Endocrinology 2011;152:2731-41.
31. Chen Y, Li X, Li B, et al. Long Non-coding RNA ECRAR Triggers Post-natal Myocardial Regeneration by Activating ERK1/2 Signaling. Mol Ther 2019;27:29-45.

Cite this article as: Shi XT, Yan LJ, Lu FY, Ye MJ, Yu P, Zhong Y, Chen JH, Hu CH, Tang QY. Exploring the therapeutic potential of simvastatin in pancreatic neuroendocrine neoplasms: insights into cell cycle regulation and apoptosis. Transl Cancer Res 2024;13(8):4315-4323. doi: 10.21037/tcr-24-363

